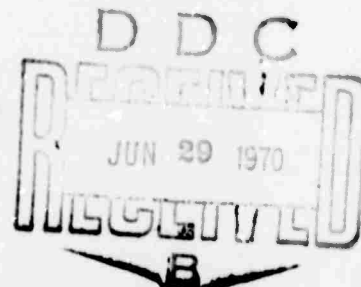


United Aircraft Research Laboratories



June 26, 1970



Director
Advanced Research Projects Agency
Washington, D. C. 20301

Attention: Col. J. M. MacCallum

Subject: Quarterly Technical Report for Contract N00014-66-C-0344
For the period 1 March 1970 to 31 May 1970

Reference: (A) Modification G06 to the subject contract dated 1 August 1969

Enclosures: (A) Three (3) copies of United Aircraft Research Laboratories
Report J920479-23

Gentlemen:

In accordance with the above modification (Reference (A)) of the subject contract, we are transmitting herewith three (3) copies of the subject report, Enclosure (A). Additional copies of this report have been distributed to the addressees on the attached distribution list.

Very truly yours,

UNITED AIRCRAFT CORPORATION
Research Laboratories

Anthony J. DeMaria
Senior Principal Scientist
Quantum Physics Laboratory

Enclosure

Reproduced by the
CLEARINGHOUSE
for Federal Scientific & Technical
Information Springfield Va. 22151

This document has been approved
for public release and sale its
distribution is unlimited.

**BEST
AVAILABLE COPY**

June 26, 1970

Director
Advanced Research Projects Agency
Washington, D. C. 20301

Attention: Col. J. M. MacCallum

ARPA Order No.: 306A#15

Program Cost Code: 9E30K21

Contractor: United Aircraft Research Laboratories

Effective Date of Contract: 1 August 1969 (Modification G06)

Contract Expiration Date: 30 July 1970

Amount of Contract: \$333,916.00

Contract No.: N00014-66-C-0344

Principal Investigator: Dr. Anthony J. DeMaria, Area Code 203, 565-3545

Project Scientist: Dr. William H. Glenn, Area Code 203, 565-5411

Short Title: Picosecond Laser Pulses

Subject: Quarterly Technical Report for the period 1 March 1970 to
31 May 1970

Reported by: A. J. DeMaria, W. H. Glenn, G. L. Lamb, Jr., M. E. Mack and E. B. Treacy

Gentlemen:

Work during this period has been concerned primarily with the development of extremely fast pumping lamps for organic dye lasers, the continuing investigation of nonlinear coherent propagation effects, the investigation of nonlinear polarization effects in Kerr active liquids and the measurement of the phase structure of picosecond pulses.

Ultrafast Flashlamps for Dye Lasers

A new approach has been taken to the problem of developing a fast rise time, short duration flashlamp for dye laser pumping. The basic circuitry involved is illustrated schematically in Fig. 1. This circuit is a modification of one designed by the National Advisory Committee for Aeronautics. (1) In operation the circuit

behaves as follows: The capacitor banks C_1 and C_2 ($C_1 = C_2$) are charged through the resistors R , r_a , and r_b . When the spark gap, S , fires the voltage, V_c , on the bank, C_2 , begins to oscillate with a frequency dependent on C_2 and L . As it does so the voltage, V_a , on the anode of the lamp begins to rise toward $+2V$ where V is the charging voltage for the circuit. If the size of the inductor, L , is chosen so that the ringing frequency of V_c is properly matched to the breakdown delay time of the lamps, the lamps can be made to fire after half a cycle, when the voltage across them is a maximum. Nearly all of the energy stored in the capacitor banks, C_1 and C_2 , is dissipated in the lamps.

This type of operation is to be contrasted to the commonly used arrangement consisting of a spark gap in series with the lamp or lamps to be fired. In such an arrangement the impedance of the spark gap limits the peak current through the lamps, often greatly reducing their light emission. The removal of the spark gap from the high frequency section of the circuitry, also facilitates the design and construction of the device. A definite improvement in rise time can be realized with the present scheme. With the more conventional single bank discharge circuit, a capacitance of $C_1 + C_2 = 2C$ is required to store the same amount of energy. In the circuit shown in Fig. 1, the capacitor banks, C_1 and C_2 , are connected in series when the lamps fire, so that the effective circuit capacitance is $C_1 C_2 / (C_1 + C_2) = \frac{1}{2}C$. Consequently, for the same amount of circuit inductance, the present design will have only half the rise time of the more conventional arrangement.

In principle any number of lamps may be used with the circuit shown in Fig. 1. It is advantageous to use more than one lamp, when more energy is required than a single lamp can safely discharge. The split capacitor bank, C_1 , assures that each lamp fires. The rapidly changing anode voltage provided by the common bank, C_2 , together with RF and UV coupling between the lamps causes the lamps to fire simultaneously. For the two lamp circuit described below, the time jitter in the firing of the lamps is negligible compared to the light output rise time.

A two joule, two lamp version of the circuit shown in Fig. 1 has been successfully tested for dye laser pumping. The circuit parameters are as follows: $R = 2 \times 10^7 \Omega$, $r_a = r_b = 10^6 \Omega$, $C_{1a} = C_{1b} = 10^{-9} \text{ f}$, $C_2 = 2 \times 10^{-9} \text{ f}$, and $L = 4 \times 10^{-7} \text{ h}$. Barium titanate insulated "doorknob" capacitors with a 30 kV rating were used to make up the capacitor banks. The spark gap could be adjusted to fire at from 25 kV to 35 kV. Figs. 2a and 2b show the lamp anode voltage with and without lamp firing. In Fig. 2a lamp ignition was prevented by increasing the lamp arc length beyond that for which breakdown could be obtained. The voltage is seen to oscillate with little damping. In Fig. 2b, where the lamps have been allowed to fire, the anode voltage returns rapidly to ground potential after approximately half a cycle, when the lamps fire. The slight overshoot is due to an energy loss from the bank, C_2 . This may either be dissipated in the triggering gap or radiated from the circuit as a result of the oscillating current.

The lamps used with this device are quartz capillary lamps with a bore of 1.2 mm and a wall thickness of 1 mm. Arc lengths of from 1.5 cm to 3.6 cm were used.

To obtain breakdown with the longer arc lengths the lamps had to be in contact with a metallic ground plate. When used to pump liquid dye solutions, the aluminum foil reflector for coupling the flashlamp light into the dye also serves this purpose. A variety of different electrodes were tried. In contrast to results with slower rise time atmospheric pressure discharges⁽²⁾ the peak light output was found to be essentially independent of the electrode material. This indicates the bulk of the discharge takes place in the original fill gas and not in material evaporated from the electrodes. The result is not surprising in light of the short time duration.

Air, nitrogen and argon have been tried as the fill gases. In all cases the light output increases with pressure over the range of from 0-3 atmospheres. The greatest light output occurs in argon; the fastest rise time, in nitrogen. Air offers nearly the same rise time as nitrogen, with nearly the same peak light output as the argon. Figure 3 shows the light output of the two lamps when filled with air at 1 atm. The peak light output and rise time are approximately constant for an arc length of from 2.0 cm to 3.2 cm. However, increasing the lamp pressure from 1 to 3 atm. nearly triples the light output in the spectral region from 2200 Å to 5000 Å, the region of sensitivity of the photodiode. At a 1 atm filling pressure the lamp radiates approximately 4×10^{-2} joule in this spectral region, giving an optical energy conversion efficiency of about 2%. Half of the radiated power is emitted between 2200 Å and 3000 Å, indicating an equivalent blackbody temperature of between 50,000°K and 100,000°K.

The 22 nsec 10% to 90% rise time shown in Fig. 3 can be reduced substantially by minimizing lead inductance in the flashlamps as shown in Fig. 4a. Here the 10%-90% rise time has been reduced to approximately 12 nsec. The half-power duration is only 50 nsec. If only one lamp rather than two is used as in Fig. 4b, the rise time is seriously degraded. This may be the result of the formation of a high inductance pinched arc. In addition, with an arc length of 2.5-3.2 cm the single lamp has a lifetime of only 10 to 50 firings at a two joule input level. At one joule per lamp in the two lamp configuration, the lamps have been fired several hundred times with no noticeable degradation in output and no sign of fracturing.

The 22 nsec rise time, one atmosphere air-filled lamps have been used to pump ethanol solutions of rhodamine 6G and fluorescein sodium. The 4 cm long, 3 mm bore dye cell was placed between the lamps in a close coupled pumping scheme using an aluminum foil reflector. The lamp arc length was 3.0 cm. With 85% reflecting output mirrors threshold was easily reached with both dyes. The dye laser outputs are shown in Fig. 5. Near threshold as in Fig. 5a, the output shows a slight initial spiking similar to that observed by Sorokin et.al. in the laser pump dyes.⁽³⁾ As the pumping intensity is increased, this initial spike increases only slightly while the remainder of the output grows rapidly. Far above threshold as in Figs. 5b and 5c the initial spike is no longer in evidence. A comparison of Figs. 5b and 5c shows little difference in the time development of the outputs with the two dyes. This indicates no appreciable triplet state quenching in the sodium fluorescein during the duration of the pumping. This is in contrast with results with longer duration flashlamps, where a very strong quenching is observed.

The output energy was quite low, being less than a millijoule in both cases. This is the result of the relatively low lamp output in the dye pump bands. The present results indicate that pressurizing the lamps to 3 atm or more should greatly improve this. Results with longer duration lamps indicate that a much higher visible region emission should be obtainable using either Xenon or krypton as the lamp fill gas. A high pressure version of the low inductance, 12 nsec rise time lamp has been fabricated and will be tested shortly for dye laser pumping.

Nonlinear Propagation Effects

The continuing work on nonlinear propagation effects has been concerned with the investigation of conservation laws governing optical pulse propagation. This work has led to a paper entitled "Higher Conservation Laws in Ultrashort Optical Pulse Propagation" by G. L. Lamb, Jr., that has been accepted for publication in PHYSICS LETTERS. This paper is included as Appendix A of this report.

Nonlinear Polarization Effects

When an intense light wave propagates through a Kerr active liquid, the intensity dependent index of refraction can lead to a variety of effects such as self-focusing, self phase modulation and steepening, and alteration of the state of polarization of the wave. It is the latter effect that is considered here. It has been known for some time that when an elliptically polarized wave propagates through such a liquid, the orientation of the axes of the ellipse are rotated by an amount proportional to the product of the fields along the major and minor axes of the ellipse and to the distance travelled.⁽⁴⁾ Recently a more detailed consideration of this effect has been undertaken and the problem has been generalized to allow for the presence of a linear birefringence such as could be produced by an externally applied dc electric field. Some preliminary results of the analyses have been reported previously. During this period the analyses has been continued and a very convenient visualization of the effects has been obtained using the Poincare sphere representation.

In the model considered, the molecules are assumed to be cylindrically symmetric with polarizabilities α_{\parallel} and α_{\perp} parallel and perpendicular to the axis of the molecule. The polarizability of the individual molecules is assumed to be linear; the nonlinearity of the macroscopic polarization results from orientation effects. If we specify the orientation of the axis of a molecule by a unit vector V , then the induced polarization is given by

$$P = (\alpha_{\parallel} - \alpha_{\perp})(E \cdot V)\bar{V} + \alpha_{\perp}E$$

and the energy of the induced dipole is then

$$\omega = -E \cdot p - (a_{11} - a_{11}) (E \cdot V)^2 + a_{11} (E \cdot E) \quad 2$$

The macroscopic polarization can then be calculated from the expression

$$P = N \frac{\int p e^{-\frac{\omega}{kT}} d\Omega}{\int e^{-\frac{\omega}{kT}} d\Omega} \quad 3$$

where N is the density of molecules and Ω the solid angle associated with V . For sufficiently small fields, $\omega/kT \ll 1$ and the exponential may be expanded in a series. The lowest order nonlinearity is obtained by retaining the first two terms in the expansion. The calculation is straightforward but rather lengthy and will not be reproduced here. The result that is obtained is

$$P = \epsilon E + \beta(I) E + P_0 \quad 4$$

Here the first term represents the ordinary linear polarization, the second term a nonlinear but isotropic polarization and the third term an anisotropic polarization. We write the optical field as

$$\mathcal{E}_{x,y} = \sum_{x_0,y_0} e^{i\Phi_{x,y}} e^{i(kz - \omega t)} \quad 5$$

The propagation direction is taken as the $+z$ direction and the applied dc field, of magnitude E_0 , defines the $+x$ direction. The anisotropic part of the polarization can then be expressed by

$$\bar{P}_0 = a \begin{bmatrix} a & b \\ -b & 0 \end{bmatrix} \begin{bmatrix} \mathcal{E}_x \\ \mathcal{E}_y \end{bmatrix} \quad 6$$

with $\frac{11}{15} \frac{(\alpha_{11} - \alpha_{11})^2}{RT}$, $a = E_0^2$ and $b = \frac{1}{4}(\epsilon_y \epsilon_x^* - \epsilon_x \epsilon_y^*)$

The behavior of the fields can be calculated from the usual slowly varying envelope approximation

$$\frac{\partial \mathcal{E}}{\partial z} = i \frac{2\pi k}{\epsilon} P_{NL} e^{-ikz} \quad 7$$

Substitution of Eq. (5) into Eq. (7) gives two coupled equations. By equating the real and imaginary parts of these equations one obtains four coupled equations for E_{x0} , E_{y0} , φ_x and φ_y . The isotropic part of the nonlinear polarization occurs only in the equation for φ_x and φ_y . This is as expected since the material is lossless and an isotropic nonlinearity should affect only the phases of the field. If we subtract the equations for φ_x and φ_y to obtain an equation for $\psi = \varphi_x - \varphi_y$, the isotropic part cancels out. Performing these operations, one obtains the following equations for E_{x0} , E_{y0} , and ψ

$$\frac{dE_{x0}}{dz} = -\frac{G}{4} E_{y0}^2 E_{x0} \sin 2\psi$$

$$\frac{dE_{y0}}{dz} = \frac{G}{4} E_{x0}^2 E_{y0} \sin 2\psi$$

8

$$\frac{d\psi}{dz} = G \int -E_0 + \frac{1}{4} (\cos 2\psi - 1) (E_{x0}^2 - E_{y0}^2)$$

where

These equations take on a much simpler form if they are expressed in terms of the Stokes parameters. To facilitate such considerations we shall first transform to the notation used in "Principles of Optics" by Bernard Wolf which contains a concise description of this topic. To this end we set

$$\phi_x = \delta_1$$

$$\phi_y = \delta_2$$

$$\psi = \delta$$

$$E_{x0} = a_1 = \sqrt{S_0} \cos \alpha$$

$$E_{y0} = a_2 = \sqrt{S_0} \sin \alpha$$

9

The Stokes parameters are then defined by

$$S_1 = a_1^2 - a_2^2 = S_0 \cos 2\alpha \quad 10a$$

$$S_2 = 2a_1 a_2 \cos \delta = S_0 \sin 2\alpha \cos \delta \quad 10b$$

$$S_3 = 2a_1 a_2 \sin \delta = S_0 \sin 2\alpha \sin \delta \quad 10c$$

$$S_0^2 = S_1^2 + S_2^2 + S_3^2 \quad 10d$$

Introducing the dimensionless length

$$\zeta = \frac{GS_0}{4} z \quad 11$$

Equation (8) becomes

$$\frac{dS_3}{d\zeta} = -rS_2 \quad 12$$

$$\frac{dS_2}{d\zeta} = -2S_2S_3/S_0 \quad 13$$

Where

$$r = 4E_0^2/S_0 \quad 14$$

Equations (12) and (13) possess the first integral

$$S_3^2 - 4E_0^2S_1 = C \quad 15$$

which is the equation for a parabolic cylinder in the S_1, S_2, S_3 space. The integration constant C is determined by E_0 and the initial values of S_1 and S_3 . Since values of the Stokes parameters are confined to the surface of a sphere of radius S_0 , the Poincaré sphere, one sees that for the present situation, the admissible states of polarization are at the intersection of the Poincaré sphere with the parabolic cylinder given by Eq. (15).

Two basically different types of intersection are possible and are indicated in Fig. 6 where the sphere is viewed from the positive S_2 axis, looking toward the origin. In Fig. 6a, $|C/4E_0^2| > S_0$ and since S_3 can never become zero, no state of plane polarization is possible. In Fig. 6b, it is possible to obtain $S_3 = 0$ and so plane polarization will be transformed into elliptical polarization. In this case the admissible polarizations are represented by a path on the surface of the sphere that is somewhat similar to the design made by the stitches on a baseball.

To determine the length of polarizing cell that is needed to affect a given change in polarization, the complete integration of Eqs. (12) and (13) must be performed. This is readily carried out in terms of elliptic functions. Using Eqs. (10d) and (15), Eq. (13) takes the form

$$\frac{dS}{d\zeta} = -\frac{2}{S_0} \sqrt{(C + 4E_0^2S)(S_{1+} - S)(S_1 - S_{1-})} \quad 16$$

where S_{1+} and S_{1-} are defined by the factorization

$$(S_{1+} - S_1)(S_1 - S_{1-}) = S_0^2 - C - 4E_0^2S_1 - S_1^2 \quad 17$$

The integration of Eq. (16) now leads to⁽⁵⁾

$$S_3 = S_1 + \operatorname{dn} \left[\frac{G}{4} S_1 + (z - z_0), k \right] \quad 18$$

where

$$k^2 = \frac{S_{1+} - S_{1-}}{S_{1+} + C/4 E_0^2} \quad 19$$

for $S_{1-} < -C/4 E_0^2$, i.e., the case shown in Fig. 6b, $k^2 > 1$ and it is convenient to use the transformation⁽⁶⁾

$$\operatorname{dn}(4, k) = \operatorname{cn}(kn, k^{-1}) \quad 20$$

One then obtains

$$S_3 = S_1 + \operatorname{cn} \left[\frac{GE_0}{2} \sqrt{S_{1+} - S_{1-}} (z - z_0), k^{-1} \right] \quad 21$$

With S_3 determined by either Eq. (18) or (21), S_1 is given by Eq. (15) and finally S_2 is obtained from Eq. (10d). From Eqs. (10b) and (10c), the angle of orientation of the ellipse is given by

$$\tan \delta = \frac{S_3}{S_2} \quad 22$$

Use of these results will be described in the next report.

Measurement of the Phase Structure of Picosecond Pulses

In the previous technical report, J920479-21, the design of an ultrafast spectrometer for the measurement of the phase structure of picosecond pulses was described and some preliminary measurements were presented. Work in this area has continued and has resulted in a paper entitled "Direct Demonstration of Picosecond Pulse Frequency Sweep," by E. B. Treacy. This paper has been accepted for publication in Applied Physics Letters and is included as Appendix B of this report. A more complete theory of the spectrometer and a general theory of measurement and interpretation of dynamic spectrograms will be presented in the next report.

J920:79-23

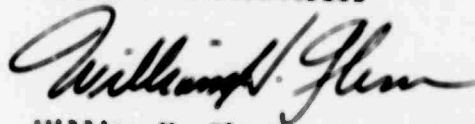
-9-

June 26, 1970

During the next reporting period, research will continue in the above mentioned areas.

Very truly yours,

UNITED AIRCRAFT CORPORATION
Research Laboratories

A handwritten signature in cursive script, reading "William H. Glenn".

William H. Glenn
Principal Scientist
Quantum Physics

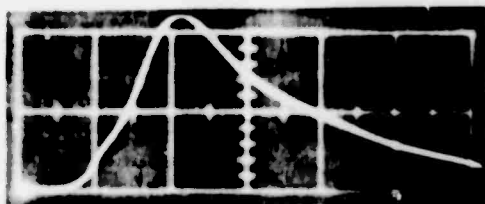
WHG:ek

REFERENCES

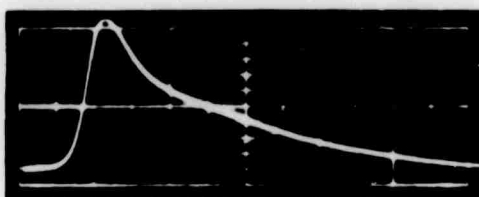
1. Lewis Flight Propulsion Laboratory, National Advisory Committee for Aeronautics, Cleveland, Ohio, NACA RM E50K27.
2. R. B. A. Frungel, High Speed Pulse Technology, Vol. II, Chapt. 4b, p. 54. (Academic Press, New York, 1965).
3. P. P. Sorokin, J. R. Lankard, E. C. Hammond and V. L. Morrizzi, I.B.M. Journal 11, 130 (1967).
4. P. D. Maker and R. W. Terhune, Phys. Rev. 137, A801 (1965).
5. P. F. Byrd and M. D. Friedman, Handbook of Elliptic Integrals. (Springer Verlag, Berlin, 1954).
6. W. Magnus and F. Oberhettinger, Formulas and Theorems for the Special Functions of Mathematical Physics. (Chelsea, New York, N.Y., 1954) 2nd Ed. p. 105.

DYE LASER OUTPUT

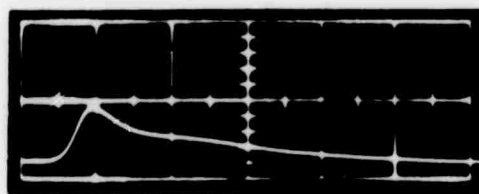
10 nsec/cm



a) SODIUM FLUORESC EIN NEAR THRESHOLD



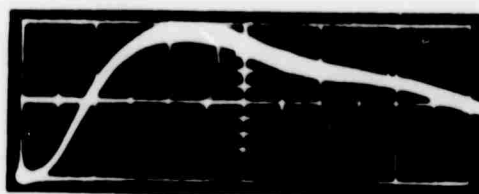
b) SODIUM FLUORESC EIN WELL ABOVE THRESHOLD



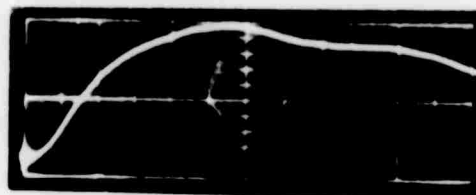
c) RHODAMINE 6G WELL ABOVE THRESHOLD

LAMP OUTPUT-MINIMUM INDUCTANCE CONFIGURATION

10 nsec/cm

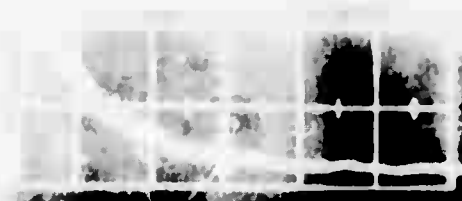


a) TWO LAMPS

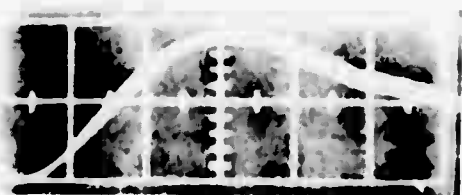


b) SINGLE LAMP

LAMP OUTPUT



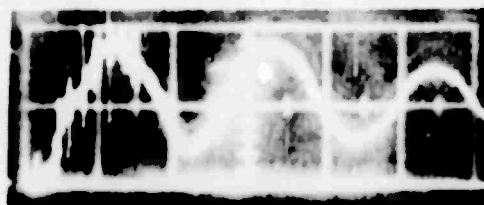
a) 50 nsec/cm



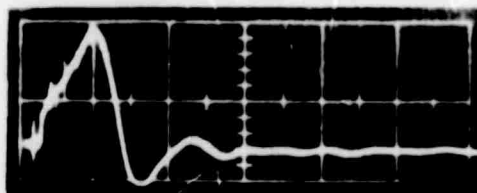
b) 10 nsec/cm

LAMP ANODE VOLTAGE- V_2

100 nsec/cm



a) LAMPS REMOVED



b) LAMPS FIRED

BASIC CIRCUITRY-TWO LAMP CONFIGURATION

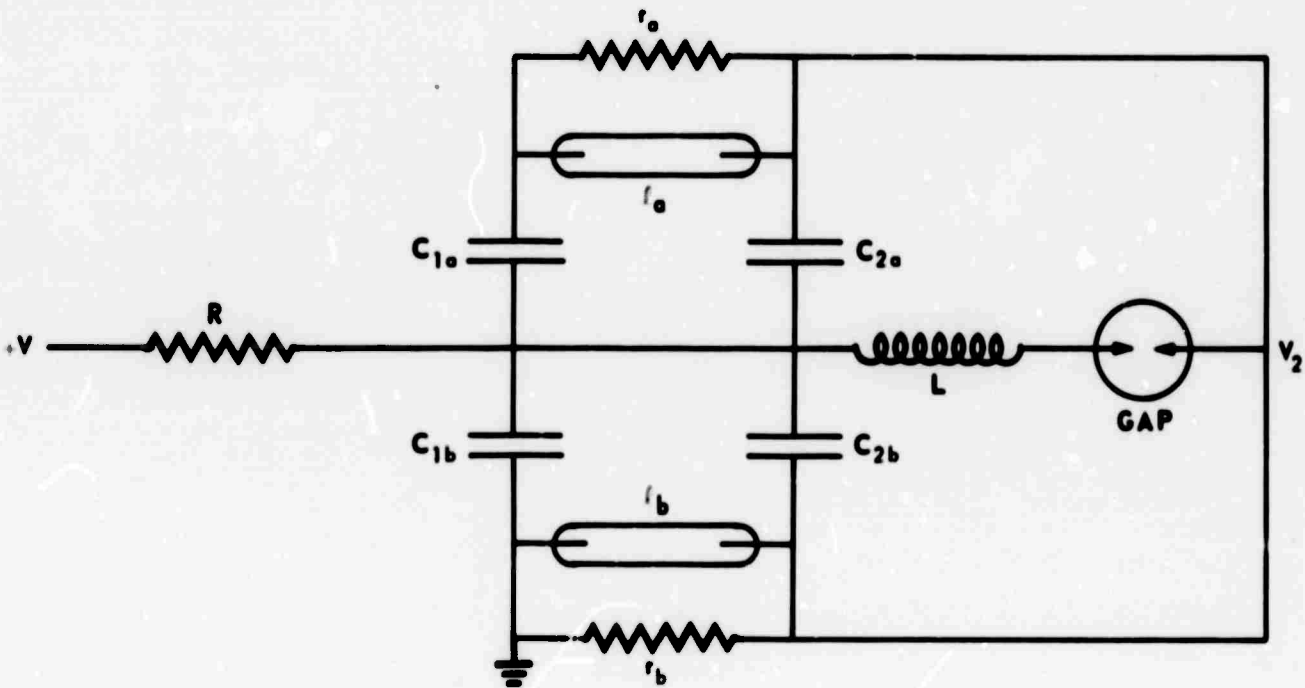
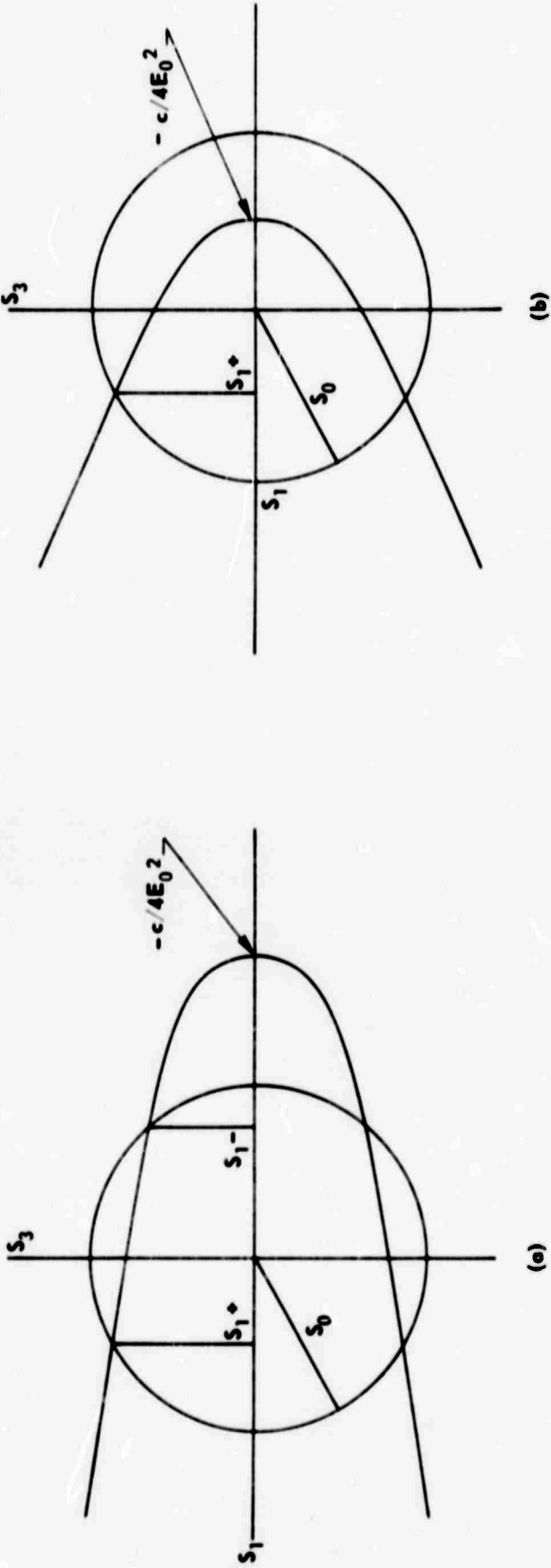


FIG. 6

INTERSECTION OF PARABOLIC CYLINDER
WITH POINCARÉ SPHERE



APPENDIX A

Higher Conservation Laws in Ultrashort Optical Pulse Propagation

G. L. Lamb, Jr.

United Aircraft Research Laboratories

East Hartford, Connecticut 06108, U.S.A.

ABSTRACT

A method for generating conservation laws associated with the propagation of ultrashort optical pulses is summarized. Two pairs of conservation laws beyond those of field energy and field momentum are presented.

It has been shown that the decomposition of a 2π optical pulse in an attenuator into $n2\pi$ pulses can be understood in terms of a simple theoretical model^(1, 2). The model provides a description of pulse propagation in terms of certain particular solutions of the equation

$$\frac{\partial^2 \sigma}{\partial \xi \partial \tau} = -\sin \sigma \quad (1)$$

The electric field envelope ξ is related to σ by $\xi = \partial \sigma / \partial \tau$ while ξ and τ are dimensionless space and retarded time variables respectively as defined in Ref. 1.

The pulse decomposition is similar to that observed in recent studies of the Korteweg-deVries equation^(3,4,5). This latter equation has been shown to possess an infinite number of conservation laws⁽⁶⁾. Such conservation laws have been found useful in determining the relative amplitudes of the various pulses into which an initial pulse may decompose^(4,5).

The similarity between solutions of Eq. (1) and those of the Korteweg-deVries equation leads one to conjecture that Eq. (1) may also possess higher conservation laws. In the present note a method for obtaining such higher conservation laws is described and two pairs of new conservation laws are given. The total number of such additional conservation laws is not considered although the method of derivation appears to admit of unlimited extension.

The usual conservation laws relating to field energy and field momentum are readily obtained by standard methods. One finds $\frac{1}{2}(\sigma_\xi^2)_\tau + (1 - \cos \sigma)_\xi = 0$ as well as the equation obtained by interchanging ξ and τ in this result. Subscripts refer to partial differentiation. By following the methods given in Refs. 4 and 5, these two conservation laws may be used to predict the amplitude of each of the 2π pulses into which a 4π pulse of the arbitrary initial shape will decompose⁽⁷⁾.

The following conservation laws obeyed by solutions of Eq. (1) have also been constructed:

$$\left(\frac{1}{4} \sigma_\xi^4 - \sigma_{\xi\xi}^2 \right)_\tau - \left(\sigma_\xi^2 \cos \sigma \right)_\xi = 0 \quad (2)$$

$$\left(\frac{1}{6} \sigma_\xi^6 - \frac{2}{3} \sigma_\xi^2 \sigma_{\xi\xi}^2 + \frac{8}{9} \sigma_\xi^3 \sigma_{\xi\xi\xi} + \frac{4}{3} \sigma_{\xi\xi\xi}^2 \right)_\tau - \left[\cos \sigma \left(\frac{1}{9} \sigma_\xi^4 - \frac{4}{3} \sigma_{\xi\xi}^2 \right) \right]_\xi = 0 \quad (3)$$

Two additional laws follow from the interchange of ξ and τ in these expressions.

The conserved densities in these results may be derived by considering Eq. (1) within a Hamiltonian framework. A Lagrangian density for Eq. (1) is $\mathcal{L} = \frac{1}{2}\sigma_\tau^2 - (1 - \cos\sigma)$. The canonical momentum is $\pi = \partial\mathcal{L}/\partial\sigma_\tau = \sigma_\tau$ and the Hamiltonian density takes the form $\mathcal{H} = (1 + \cos\sigma)$. Recalling that a function, f , defined by $f(\tau) = \int d\xi \mathcal{F}(\sigma, \sigma_\xi, \pi, \pi_\xi)$, has a time derivative given by

$$\dot{f} = \int d\xi \left(\frac{\delta \mathcal{F}}{\delta \sigma} \frac{\delta \mathcal{H}}{\delta \pi} - \frac{\delta \mathcal{H}}{\delta \sigma} \frac{\delta \mathcal{F}}{\delta \pi} \right) \quad (4)$$

where the symbol δ refers to the variational derivative, one sees that in the present instance the conservation of f requires

$$\int_{-\infty}^{\infty} d\xi \frac{\delta \mathcal{F}}{\delta \pi} \sin \sigma = 0 \quad (5)$$

The conserved density given in Eq. (2) is recovered from this result by first noting that it is of the form $\mathcal{F}(\pi, \pi_\xi)$. Secondly, the vanishing of the integrand in Eq. (5) will be assured if it is of the form $\partial G / \partial \xi$ where $G(\sigma, \pi, \pi_\xi)$ vanishes at $\xi = \pm \infty$. This leads to the partial differential equation

$$\left[\frac{\partial \mathcal{F}}{\partial \pi} - \frac{\partial}{\partial \xi} \left(\frac{\partial \mathcal{F}}{\partial \pi_\xi} \right) \right] \sin \sigma = \frac{\partial G}{\partial \xi} = \frac{\partial G}{\partial \sigma} \pi + \frac{\partial G}{\partial \pi} \pi_\xi + \frac{\partial G}{\partial \pi_\xi} \pi_{\xi\xi} \quad (6)$$

This equation is readily solved and the form of G determined. The method used is outlined below in the consideration of Eq. (3). Neglecting terms which have the form of an exact divergence or correspond to the lower conservation laws pertaining to field energy or field momentum one obtains

$$\mathcal{Q} \sim \pi^4 - \pi_\xi^2 \quad (7)$$

which is the density given in Eq. (2).

The method may also be used to derive Eq. (3) but a somewhat more direct approach is to avoid the partial integrations employed in the derivation of Eq. (4) and set

$$\frac{\partial \mathcal{F}}{\partial \pi} \pi_\tau + \frac{\partial \mathcal{F}}{\partial \pi_\xi} \pi_{\tau\xi} + \frac{\partial \mathcal{F}}{\partial \pi_{\xi\xi}} \pi_{\tau\xi\xi} = \frac{\partial G}{\partial \xi}(\sigma, \pi, \pi_\xi) \quad (8)$$

Recalling that $\pi_\tau = \frac{1}{2}\sin\sigma$, and noting from the structure of Eq. (8) that $G = A(\pi, \pi_\xi) \cos\sigma + B(\pi, \pi_\xi) \sin\sigma$ while \mathcal{F} is at most quadratic in $\pi_{\xi\xi}$, one obtains the result given in Eq. (3).

This research was supported by the Advanced Research Projects Agency of the Department of Defense and was monitored by the Office of Naval Research under contract No. N00014-66-C-0344.

REFERENCES

1. G. L. Lamb, Jr., Phys. Letters 25A (1967), 181.
2. G. L. Lamb, Jr., in: In Honor of Philip M. Morse, edited by H. Feshbach and K. U. Ingard (M.I.T. Press, 1969), 88.
3. N. J. Zabusky and M. D. Kruskal, Phys. Rev. Letters 15 (1965), 240.
4. N. J. Zabusky, in Nonlinear Partial Differential Equations, edited by W. F. Ames (Academic Press, New York, 1967), 223.
5. V. I. Karpman and V. P. Sokolov, Soviet Physics JETP 27 (1968), 839.
6. R. M. Miura, C. S. Gardner and M. D. Kruskal, J. Math. Phys. 9 (1968), 1204.
7. G. L. Lamb, Jr., in Proceedings of the Rochester Symposium on Electromagnetic Interactions of Two-Level Atoms, edited by J. H. Eberly (University of Rochester, 1970), 37.

APPENDIX B

Direct Demonstration of Picosecond Pulse
Frequency Sweep*

E. B. Treacy

United Aircraft Research Laboratories

East Hartford, Connecticut 06108

ABSTRACT

A direct measurement using time-resolved spectroscopy with response times in the picosecond regime shows that wave groups of different frequencies within an ultrashort pulse generated by a Nd:glass mode-locked laser arrive at a given point at different times. A curve depicting wavelength versus arrival time for a typical pulse is constructed. The frequency sweep is nonlinear and positive across the most intense portion of the spectrum.

* This work was supported in part by the Advanced Research Projects Agency of the Department of Defense and was monitored by the Office of Naval Research under Contract No. N00014-66-C-0344.

Direct Demonstration of Picosecond Pulse

Frequency Sweep*

E. B. Treacy

United Aircraft Research Laboratories

East Hartford, Connecticut 06108

Previous measurements of the structure of picosecond pulses from a mode-locked Nd:glass laser using compression techniques^(1,2) demonstrated the existence of phase modulation. The technique permitted detection of only the positive linear frequency sweep component, and it was not possible to deduce for example whether the carrier frequency sweep was sometimes negative⁽³⁾. Although several linear⁽⁴⁾ and nonlinear⁽³⁾ optical effects are assumed to contribute to the phase modulation, identification of the dominant contributing mechanisms would be aided by a more complete knowledge of the phase structure.

The present paper discusses the direct measurements of sweep rate as a function of wavelength across approximately 115 Å of the laser spectrum at 1.06 microns. By averaging these measured rates over several shots of the laser at each of the selected wavelengths and integrating it is possible to construct a curve of wavelength versus time in a typical pulse. The measurements were made on a Nd:glass mode-locked laser of conventional construction⁽⁵⁾, and the data were taken from essentially the entire cross section of the laser output beam. The whole pulse train from the laser was used in the experiments and as a result the known pulse-to-pulse variations⁽²⁾ throughout the train degrade the individual measurements. Any particular pulse may have phase structure considerably different from that of the "typical" pulse⁽⁶⁾, but the dominant feature of these results is a positive frequency sweep in the most intense region of the spectrum.

An optical pulse can be represented in the frequency domain by a complex Fourier amplitude

$$g(\omega) = |g(\omega)| e^{i\phi(\omega)}$$

where both the amplitude and phase factors determine the amplitude and phase modulation of the pulses. Ordinary spectra give $|g(\omega)|^2$ and lose the $\phi(\omega)$ information, so that one cannot positively identify a modulation of $|g(\omega)|^2$ as a phase modulation effect (such as a frequency sweep⁽⁷⁾) in contrast to amplitude modulation. As an example, suppose that the pulse represented by the spectrum $|g(\omega)|^2$ is passed through a pulse compressor^(8,9). The amplitude and phase modulations might be transformed drastically without any change in $|g(\omega)|^2$. The present technique

sacrifices some information on $|g(\omega)|^2$ to provide partial information on $\phi(\omega)$, and in fact can demonstrate a frequency sweep directly; although it cannot tell just how smooth the frequency sweep is.

The basic principle of the experiment is that of time-resolved spectroscopy. The spectrometer construction will be described elsewhere, together with a more complete discussion of these and other measurements made with it. For the present purposes, it is sufficient to note that it has a response in its focal region that approximates that of a continuum of $\sim 20 \text{ cm}^{-1}$ wide filters spanning the frequency band and spatially dispersed to the extent of 14.2 \AA per mm. The response time is approximately 2 psec, which is less than the duration of the optical pulses being measured. When a frequency-swept pulse passes through the spectrometer its different frequency components cross the focal plane at different times. The sweep rate is obtained by measuring the differential arrival times between different frequency components in the focal region. This is accomplished by a modification of the standard two-photon absorption fluorescence (TPF) technique⁽¹⁰⁾ as illustrated in Fig. 1. The focus of the spectrometer is located in the center of the fluorescent dye cell. The pulse crosses an inverted image of itself, and because the wavelength increases in opposite directions in the two members as shown in the figure, the TPF display will be tilted for a chirped pulse. Figure 1 shows directly the positive frequency sweep; i.e., longer wavelengths arriving at the focus earlier than shorter wavelengths.

When the TPF is photographed the region of enhanced fluorescence gives the antisymmetrized dynamic spectrogram

$$\tau(\omega_0 + \Delta\omega) - \tau(\omega_0 - \Delta\omega)$$

where $\tau(\omega)$ is the arrival time of the group ω . Because of the variation of TPF intensity across the pulse spectrum, this function cannot easily be followed to very large $\Delta\omega$, but the slope of the TPF at the center gives the sweep rate at ω_0 . The frequency ω_0 that intersects itself in the focal plane is readily adjusted by moving the beams, as is obvious by reference to Fig. 1, and it is determined by measuring the distance between the beams in the focal plane with a 10 \AA wide interference filter in front of the spectrometer. (It should be noted that $\omega_0 + \Delta\omega$ will combine with $\omega_0 - \Delta\omega$ to give two-photon absorption at $2\omega_0$ even if $2(\omega_0 + \Delta\omega)$ lies outside the two-photon absorption band, so that the present method of using TPF for pulse studies is capable of providing information on pulses having greater bandwidth than the two-photon absorption⁽¹¹⁾.)

The sweep rate has been measured at various wavelengths across the laser spectrum and the results are shown in Fig. 2. Each point is the average of several shots of the laser. The r.m.s. spread shown at each point indicates the shot to shot variation in measured slopes. The spectrum is most intense at $10,580 \text{ \AA}$ and there the

sweep rate is always positive (carrier frequency increasing with time). A reverse sweep is sometimes noted at the ends of the spectrum, and is more often seen at the short wavelength end. When this happens, it means that two carrier frequencies are present (and changing) simultaneously, and the beating of these components would modulate the pulse envelope. We have never observed a negative frequency sweep preceding or following the positive sweep with the laser mode-locked in the conventional way.

Figure 3 shows the "typical" pulse chirp characteristic obtained by integrating the average rates of Fig. 2. A pulse with this characteristic would have a duration of about 5 psec within the bandwidth shown, with its peak near 3 psec where the spectrum is peaked. (Whether it would exhibit appreciable sub-picosecond amplitude structure⁽¹²⁾ depends on whether the minimum observable group length is comparable to the pulse duration,⁽¹³⁾ and whether wave groups with widely differing carrier frequencies are simultaneously present. Although present indications are that this is not so with the laser studied here, experiments on amplified single pulses may give more direct information.) Since the curve of Fig. 3 has one inflexion point, the pulse would compress to either a single pulse or a multiplet on passing through a grating pair,⁽⁹⁾ depending on whether the group delay dispersion was greater or less than approximately 8 psec per 100 Å.

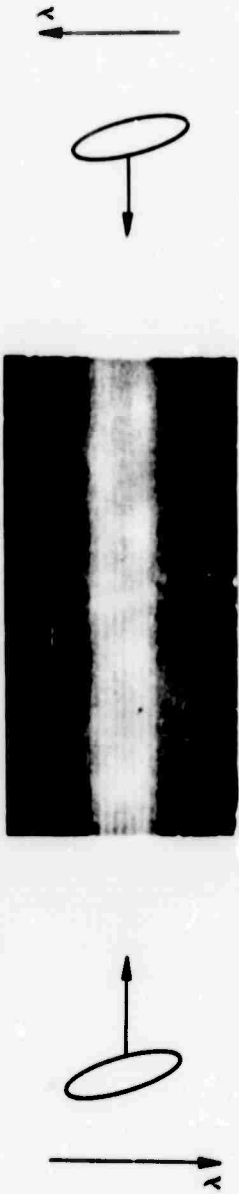
List of References

1. E. B. Treacy, Phys. Letters 28A, 34 (1968).
2. E. B. Treacy, Appl. Phys. Letters 14, 112 (1969).
3. Such effects could be caused by self-phase modulation occurring (a) in the chlorobenzene used as the mode-locking dye solvent; see for example F. DeMartini, C. H. Townes, T. K. Gustafson and P. L. Kelley, Phys. Rev. 164, 312 (1967) and R. A. Fisher, P. L. Kelley, and T. K. Gustafson, Appl. Phys. Letters 14, 140 (1969); or (b) in the glass; see M. A. Duguay, J. W. Hansen, and S. L. Shapiro "Study of the Nd:glass Laser Radiation by Means of Two-Photon Fluorescence" IEEE J. Quantum Electronics (to be published).
4. Examples are normal and anomalous dispersion in the glass and in the dye cell. Normal dispersion is considered by Rinaldo R. Cubeddu and Orazio Svelto, IEEE Jl. Quant. Elect. QE-5, 495 (1969).
5. The glass was American Optical Type 850 which had been re-annealed after extensive use. The laser was mode-locked with Eastman 9740 dye dissolved in chlorobenzene.
6. The weighting function across the pulse train that governs the measurement at any one wavelength may be wavelength dependent.
7. R. R. Alfano and S. L. Shapiro, Phys. Rev. Letters 24, 592 (1970).
8. F. Gires and P. Tournois, Compt. Rend. Acad. Sci. (Paris) 258, 6112 (1964). See also M. A. Duguay and J. W. Hansen, Appl. Phys. Letters 14, 14 (1969).
9. E. B. Treacy, IEEE Jl. Quant. Electronics QE-5, 454 (1969).
10. J. A. Giordmaine, P. M. Rentzepis, S. L. Shapiro and K. W. Wecht, Appl. Phys. Letters 11, 216 (1967). See also A. J. DeMaria, W. H. Glenn, M. J. Brienza, and M. E. Mack, Proc. IEEE 57, 2 (1969).
11. The two-photon absorption spectrum of the Rhodamine 6G in ethylene dichloride used here has not yet been measured.
12. S. L. Shapiro and M. A. Duguay, Phys. Letters 28A, 698 (1969).
13. A sharp edge or spike in the envelope would contribute to the spectrogram a time-independent feature with large bandwidth.

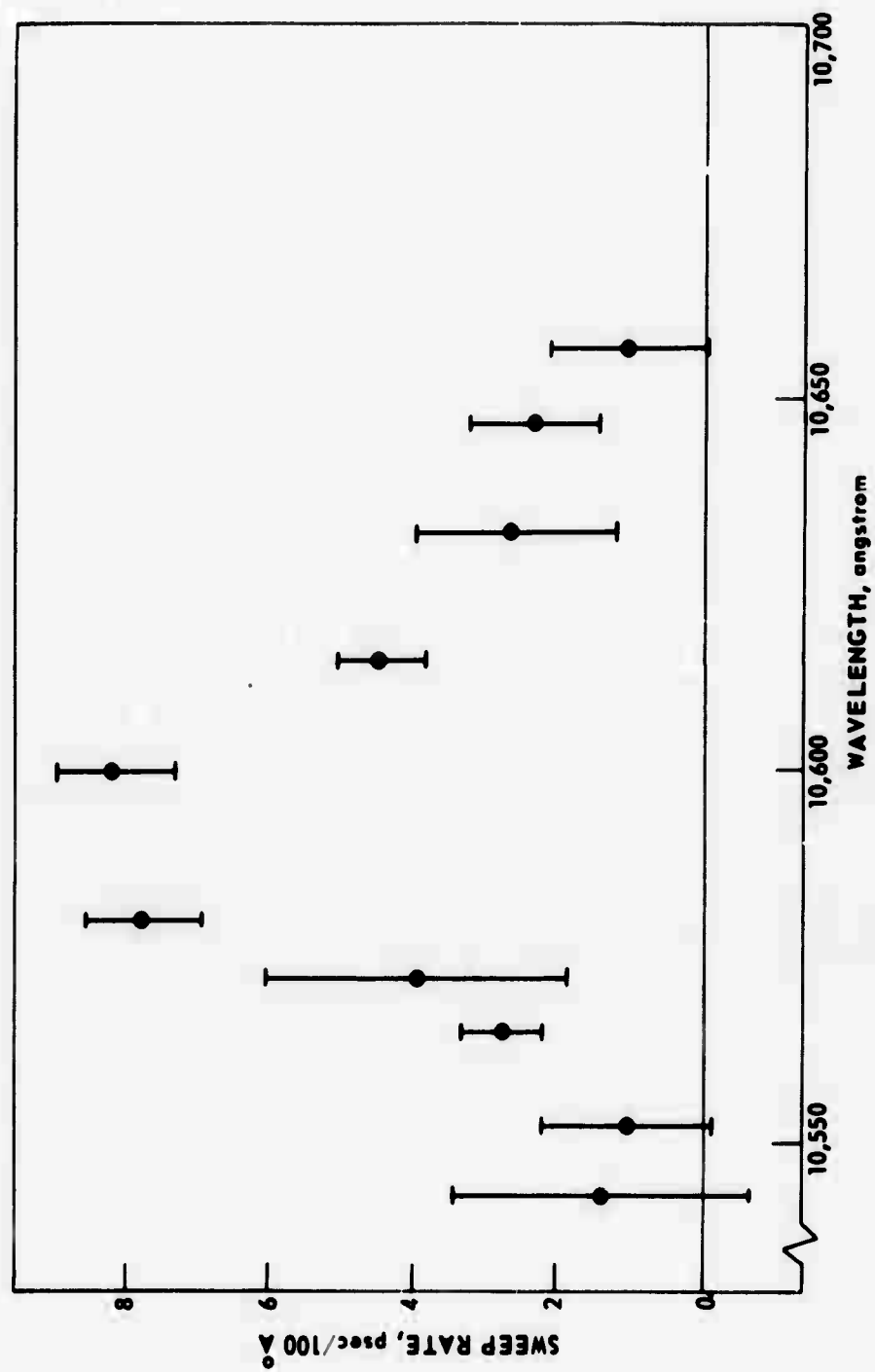
Captions for Figures

1. TPF showing the tilted display expected for a chirped pulse. Here the longer wavelength components arrive in the focal region before the shorter wavelengths. Note that wavelength increases in the upward direction for the pulse on the right and in the downward direction for the pulse on the left.
2. Sweep rates obtained by measuring the slopes on displays like that of Fig. 1.
3. The sweep characteristics of a typical pulse. The data were taken over the complete pulse trains from many laser shots, and across the whole cross section of the laser beam as explained in the text.

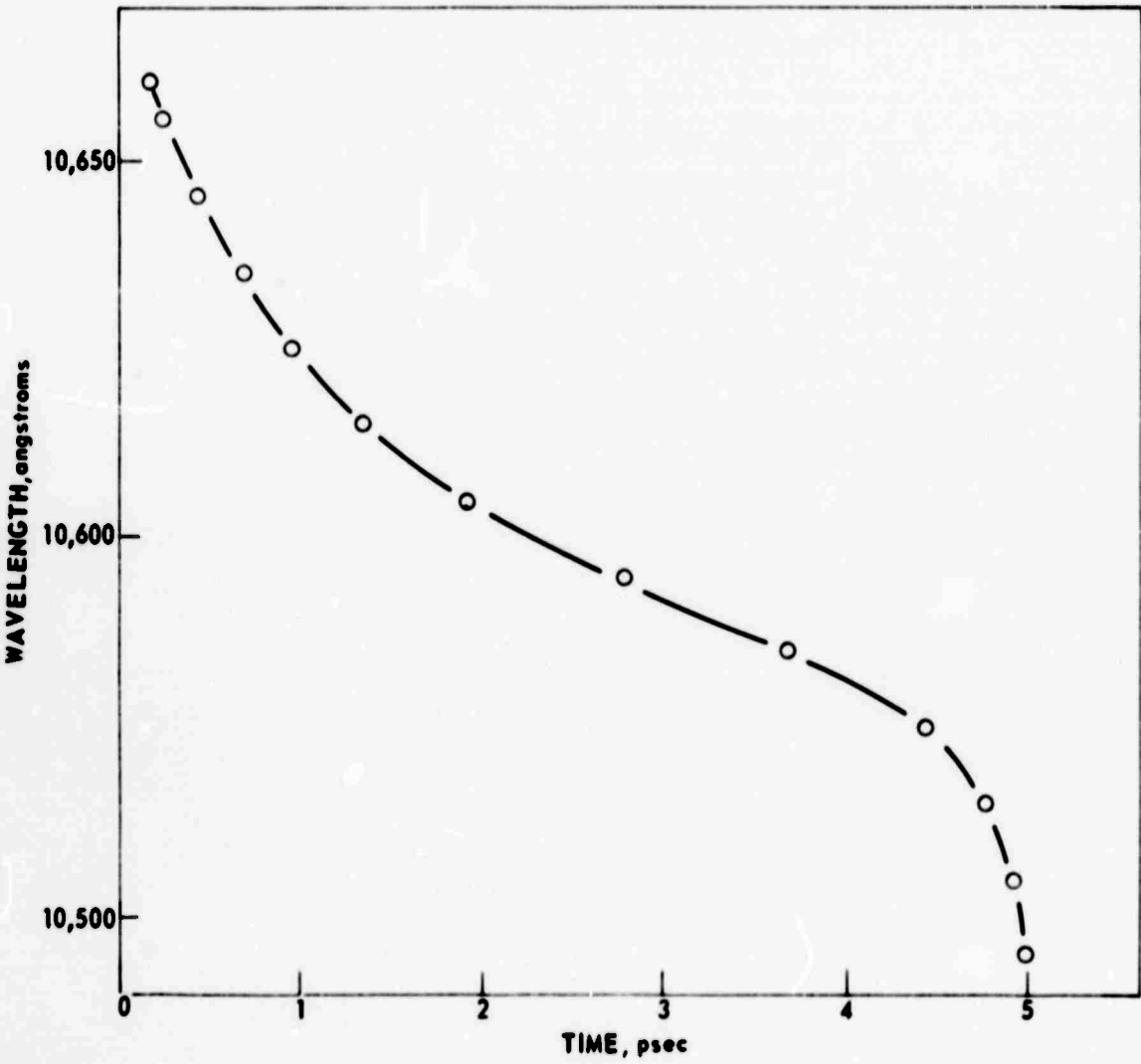
TPF CHIRPED PULSE DISPLAY



MEASURED CHIRP RATE



PICOSECOND PULSE CHIRP CHARACTERISTICS



UNCLASSIFIED

Security Classification

DOCUMENT CONTROL DATA - R & D

(Security classification of title, body of abstract and indexing annotation must be entered when the overall report is classified)

1. ORIGINATING ACTIVITY (Corporate author) United Aircraft Corporation Research Laboratories East Hartford, Connecticut 06108		2a. REPORT SECURITY CLASSIFICATION UNCLASSIFIED	
		2b. GROUP	
3. REPORT TITLE Research Investigation of Picosecond Laser Pulses			
4. DESCRIPTIVE NOTES (Type of report and inclusive dates) Quarterly Technical Report for the period 1 March 1970 to 31 May 1970.			
5. AUTHOR(S) (Print name, middle initial, last name) Anthony J. DeMaria, William H. Glenn, George L. Lamb, Jr., Michael E. Mack, E. Brian Treacy			
6. REPORT DATE June 26, 1970		7a. TOTAL NO. OF PAGES 35	7b. NO. OF REFS 26
8a. CONTRACT OR GRANT NO N00014-66-C-0344		8b. ORIGINATOR'S REPORT NUMBER(S) J920479-23	
b. PROJECT NO			
c.		9a. OTHER REPORT NO(S) (Any other numbers that may be assigned this report)	
d.			
10. DISTRIBUTION STATEMENT Reproduction in whole or in part is permitted for any purpose of the U. S. Government			
11. SUPPLEMENTARY NOTES		12. SPONSORING MILITARY ACTIVITY Advanced Research Projects Agency Monitored by the Office of Naval Research	
13. ABSTRACT This report describes experimental investigations of fast pumping sources for organic dye lasers, analytical investigations of nonlinear propagation effects in Kerr active liquids, analyses of coherent propagation effects and investigations of the phase structure of picosecond pulses.			

Picosecond Laser Pulses

Nonlinear Propagation Effects

Organic Dye Lasers

Flashlamp Design